FINAL PROJECT RESULTS

FOR

U.S. NAVAL FACILITIES ENGINEERING SERVICE CENTER
560 CENTER DRIVE
PORT HUENEME, CA 93043-4328 USA

IN PARTIAL FULFILLMENT OF ONR GRANT N00014-95-1-0828

LOCATION OF ORDNANCE-LIKE OBJECTS IN COASTAL WATERS TO DEPTHS OF 50 METERS

PREPARED BY:

CHARLES L. MORGAN, PH.D.
ASSOCIATE DIRECTOR
MARINE MINERALS TECHNOLOGY CENTER
UNIVERSITY OF HAWAI'I
811 OLOMEHANI STREET
HONOLULU, HI 96813-5513
TEL: (808) 522-5611 • FAX: (808) 522-5618
E-MAIL: SAUCHAI@AOL.COM

JUNE 30, 1996

TABLE OF CONTENTS

LIST OF TABLES

LIST OF FIGURES

LOCATION OF ORDNANCE-LIKE OBJECTS IN COASTAL WATERS TO DEPTHS OF 50 M

INTRODUCTION

Many coastal marine sites in the tropical Pacific and elsewhere were the sites of intensive fire fights during World War II, and others were subsequently used over extended periods by the U.S. armed services and allies as training areas for simulated warfare using live ordnance. The reduction of defense needs has resulted in the termination of many of these activities and some of the islands and their surrounding environs are scheduled to be cleaned up and returned to public use.

Identified ordnance discarded in offshore areas includes naval shells, bombs, rockets, torpedoes, mortar rounds, and small arms ammunition, much of it unexploded and some of it buried upon impact or subsequently by sedimentary processes. In some sites the Navy has delineated a 2-mile danger zone around the coast, but it is generally understood that areas designated for immediate clean-up extend only to the 50-meter isobath, since common usage of the seabed, and the associated risks of interactions with such objects, do not extend significantly to deeper waters except for the occasional deep-water fishing trawler.

The Marine Minerals Technology Center (MMTC) has for the last six years been developing techniques for quantitative mapping of seabed mineral deposits. An important class of seabed minerals is the placer deposit, consisting of concentrations of relatively dense minerals, such as gold, tin, and others, which are sorted naturally by wave and current action into shallow seabed accumulations. These deposits are generally not easy to find and exploit because they are small and their occurrence is notoriously difficult to predict using available geological and engineering models.

This pursuit has led MMTC to develop a number of tools and techniques which can be used with relatively small investment to improve the odds of finding and mapping these deposits. In key respects, placers are similar to ordnance in that they are smaller than most geological structures and consist of anomalous concentrations of specific materials in sites which are not easy to predict. The methods developed by MMTC and their collaborators for placers can provide cost effective means for finding and classifying ordnance. The objective of this project is to demonstrate this technology on an appropriate scale to facilitate their removal, destruction, or other remediation.

ORGANIZATION

The project was completed using the talents and facilities of the following groups, organized as follows.

The **Marine Minerals Technology Center, Ocean Basins Division** (MMTC/OBD) is a part of the Center for Ocean Resource Technology under the Hawai'i Natural Energy Institute within

the School of Ocean and Earth Science and Technology at the University of Hawai'i. Its Associate Director, Dr. Charles L. Morgan, served as Principal Investigator of this project and worked closely with the co-investigator, Dr. Michael J. Cruickshank, Director of MMTC/OBD, to oversee all aspects of the work. MMTC provided all the equipment, through former acquisition, lease or purchase, to complete the project. MMTC/OBD is responsible for all deliverables to the Naval Facilities Engineering Service Center (NFESC) and for the management of the following project team members.

Oceanic Imaging Consultants (OIC) is an independent consulting firm located at the Manoa Innovation Center in Honolulu, Hawai'i. OIC subcontracted directly with MMTC/OBD to develop and test the the side-scan sonar system and to generate the primary target location and classification predictions using all available data.

The **Marine Minerals Technology Center, Continental Shelf Division** (MMTC/CSD), is the affiliated academic research center with MMTC/OBD and is located at the University of Mississippi. MMTC/CSD subcontracted directly with MMTC/OBD for its participation in this project. Mr. Douglas Lockhart, Senior Staff Engineer for MMTC/CSD, worked closely with Dr. J. Robert Woolsey, Director of MMTC/CSD is reporting directly to MMTC/OBD. MMTC/CSD provided the differential GPS navigation and sub-seafloor reflection profiling system.

This report summarizes the key results of this project, and it presents recommendations for future work in this area. The systems evaluated include the following:

1. Navigation and location tools, specifically the differential global positioning system (DGPS) supplied by NFESC, Nautronix® short-baseline system, and Winfrog® integration software, as well as the leased TSS® ship-motion compensator.

2. Reson® SeaBat® multi-channel shallow bathymetric mapping system.

3. MMTC side-scan sonar system which includes: 1) the EdgeTech (formerly EG&G) EG&G DF-1000® 100 kHz and 500 kHz towfish and digital conversion unit and 2) two data acquisition systems (the GEODAS, supplied on a Sun® workstation platform by OIC, and the Elics® Delph Sonar program on a PC-compatible computer supplied by MMTC/CSD.

4. Advanced Airborne Hyperspectral Imaging System (AAHIS), supplied by the contractor SETS Technology, Inc.

5. Fisher® Pulse 12® time-domain electromagnetic pulse sensor, provided by MMTC/OBD.

6. Sea Engineering, Inc.®/Precision Signal® broadband, frequency modulated "chirp" shallow-reflection sonar profiler, as received both by the system itself and by the MMTC/CSD surface acoustic array.

7. The EG&G® GeoPulse® impulse reflection profiler sound source, as received by the MMTC/CSD array.

The original project schedule was to have produced three reports: 1) a quick look assessment due immediately following the at-sea activities in August, 2) a list of final target identifications and locations, as well as a transfer of the complete set of target locations and identifications to MMTC by the end of October, and a final report of the project, which was due by December 31, 1995. Technical problems ensued (see below), and MMTC was not able to deliver the quick-look or the final report as planned. As a result, a no-cost extension was granted to MMTC allowing more time for analyzing the survey results to address the major project goals of assessing conventionally available systems for potential use for unexploded ordnance (UXO) location and classification.

Included for each system are: 1) a description with the operational configuration used in the survey; 2) the principal investigator's current overall assessment of the system capabilities to address the project objectives and where appropriate, examination of the discrepancies between the results of the survey and the actual locations and classifications of the targets deployed by NFESC; 3) descriptions of data products delivered; and 4) relevant operational notes.

NAVIGATION SYSTEMS

System Description

All of the navigation data collection systems used on this vessel were owned by NFESC, and were operated by Pelagos or MMTC personnel during the MMTC operations. The primary surface navigation system used on the *M/V American Islander* during the range operations was of Novatek Model #311R global positioning system (GPS) receiver, used in differential mode (DGPS). A Nautronix S04 ultra-short baseline (USBL) acoustic tracking system (ATS) was the primary system used for subsurface navigation and object tracking. Acoustic USBL beacons were used on demonstration hardware for subsea tracking. A KVH model 314AC azimuth digital compass provided ship-heading information.

Pelagos Winfrog® integrated navigation software was used on a project computer to integrate surface navigation, subsurface navigation and tracking, and compass data for real-time display and documentation. Navigation and target spreadsheet data were saved to computer hard drive and diskettes periodically during each day of operations. Navigation data were reported directly from the NFESC navigation computer to the MMTC data collection systems.

Overall Assessment

With one important exception, these systems performed very well and provided the necessary data for target location. The DGPS performed flawlessly with no significant downtime. Ship and airplane positions collected are believed to be accurate to <5 m, based upon positions retrieved on the beach at known locations. The ship-motion compensator also performed well and greatly improved the quality of the bathymetric data obtained, with some phasing problems, noted below. The navigation integration software proved to be well designed and capable of efficiently collecting and reducing the key navigation data and reporting the reduced results to

all of the data acquisition platforms. The navigation consultants from Pelagos® Corporation did an outstanding job in implementing the collection and reporting procedures on the ship as well as assisting in the interfacing of the DGPS system with the SETS Technology, Inc. airborne system.

Unfortunately, as discussed below in the operational notes for navigation and again more specifically for each sensor, the USBL did not interface well with the acoustic sensors and placed severe limits on the navigational accuracy of corresponding results for these systems.

Data Analysis

Analysis of the navigation data will be addressed below for each system. MMTC recorded the primary satellite range data, ship motions, and USBL-generated offsets as well as the inferred target locations.

Operational Notes

1. Significant acoustic cross-talk was observed between the USBL transponder signal and the side-scan receivers, causing unacceptable noise on the side-scan records and precluding continuous operation in the transponder mode.

2. In the responder mode, poor tracking of the deployed system was observed, particularly when the system was close to the ship in shallow water depths. Some signal responses were obtained in the relatively deep deployments.

3. No offsets could be determined with the USBL system for the surface-towed acoustic hydrophone arrays.

MULTI-CHANNEL BATHYMETRIC MAPPING

System Description

Bathymetry was obtained using the Reson, Inc. SeaBat® 9001 Multibeam Bathymetric Sonar System. This is the most compact, light-weight multi-channel sonar currently available on a commercial lease. It surveys over a swath of 90° across track (45° above vertical to port and starboard) with individual beam widths of 1.5°. It can be operated either from a towed or hull-mounted platform, and can be used in shallow water in water depths >5 m to 600 m. To accommodate for the motions of the survey vessel, TSS, Inc. pitch, roll, and heave sensors were also deployed simultaneously. The equipment and its use in this survey were all conventional.

Overall Assessment

The SeaBat® produced excellent bathymetric data which were readily integrated into the acquisition process. The data are very consistent from line to line and appear to be accurate to

within about 2-m water depth, with horizontal resolutions of a few meters. The system is a good complement to the side-scan sonar, producing quantitative data to remove some of the ambiguity of the time-series returns received by the side-scan system.

Data Analysis

OIC developed a logging/processing package for real-time integration of sonar, attitude and navigation data. The same package was used in post-processing to re-process the data for elimination of outliers and attitude-induced artifacts. Three problems had to be dealt with in re-processing the multibeam data: multiples and noncoherent noise, aberrant attitude and a lag between attitude and sonar data.

Multiples and random noise manifested themselves as large "delta-function" offsets in the cross-track bathymetry profits. While isolated spikes were thought to be due to noise in the water, the multiples were the result of echoes from previous pings "wrapping around" into the current "ping," obfuscating real arrivals and adding > 20m of coherent error to the data. Multiples corrupted approximately 10 to 15 percent of the data, and could probably be avoided in the future by more aggressive system-gain adjustments.

The attitude package supplied with the multibeam provided pitch, roll, and heave measurements for the vessel, which were to be used to correct the raw multibeam data to produce final bathymetry profiles. While in general this system performed admirably, as indicated by the quality of our final bathymetry, it would from time to time drift significantly, providing roll and pitch values in excess of 20 degrees, and heave in excess of 5 meters. Given the sheltered nature of the survey, and the participants recollections, such variations seemed unlikely, and required that we add an ability to mark such degraded data "bad".

Finally, while most of the attitude and sonar data were usable, it became apparent that they were not arriving at the same time. On average, attitude appeared to lag the sonar data by 3 to 6 pings, which if uncompensated would have resulted in the application of the wrong attitude correction. The bathymetric data presented here have been adjusted to accommodate for this effect by applying appropriate time delays to the data.

Folio No. 1 and Figure 1 present the resultant bathymetry from this analysis. Those interested in either using the multibeam data or making further plots are referred to the digital data contained on the survey summary tape provided with this report, in the directory BATHY, where we provide digital contours, gridded data in GMT.grd format, and ASCII XYZ files of UTM Easting/Northings and depth in meters.

Operational Notes

Though this system is much more efficient than single-channel bathymetric mappers, it should be noted that it has a much smaller swath width than side-scan systems. Since its area of coverage is confined to a 90° angle below the ship, it covers relatively small areas, particularly

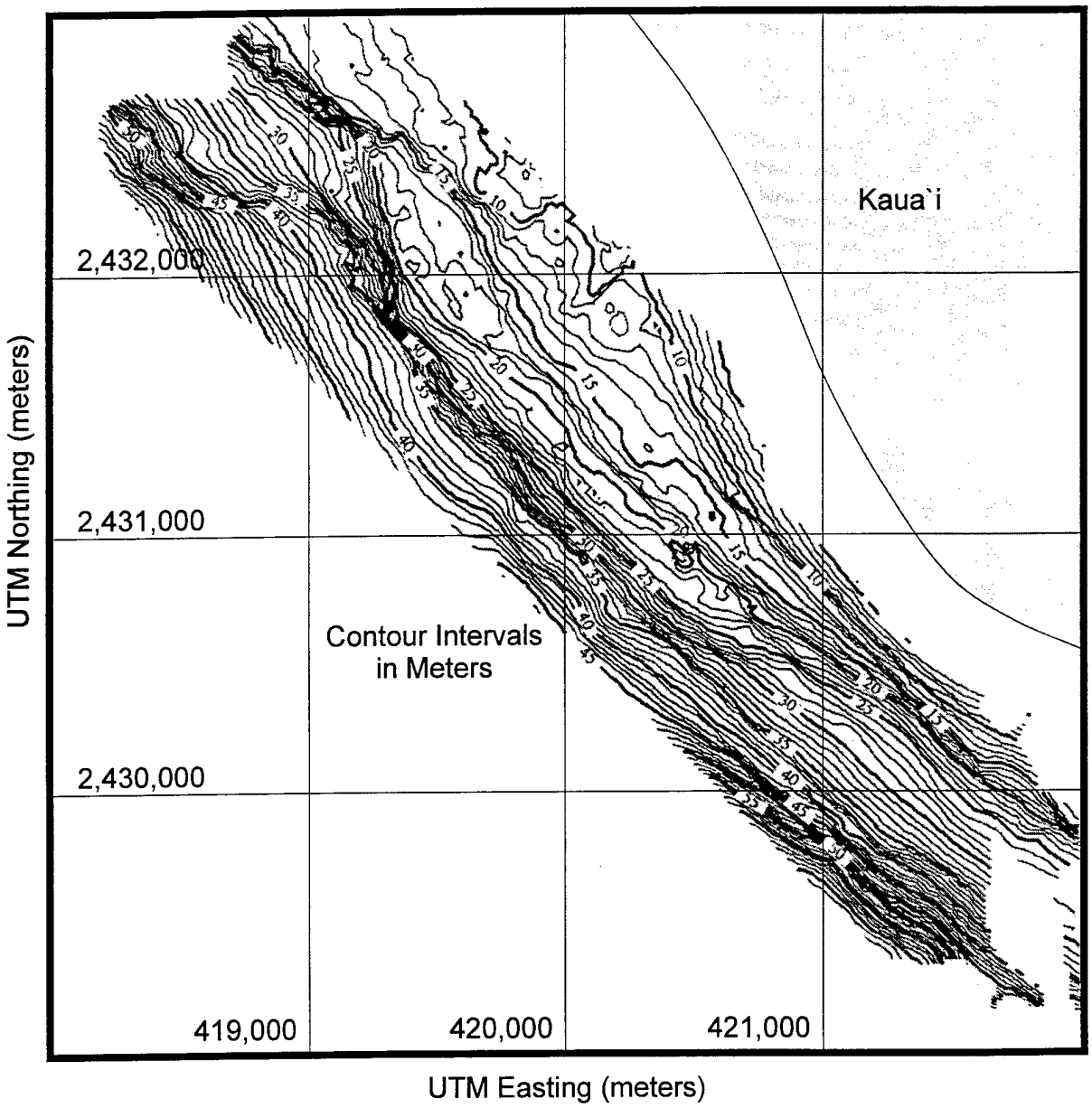

Figure 1. Test Range Bathymetry

in shallow water. It was not possible to retrieve saturation coverage in the test range, and bathymetric depths are inferred between swaths in the shallow half of the range. Two small areas of unconsolidated sediments were inferred from the records with low backscatter amplidutes. These two areas were used for the subsequent shallow-reflection profiling surveys.

SIDE-SCAN SONAR SYSTEM

System Description

This system consists of an EG&G® DF-1000 digital, dual frequency (100 and 500 kHz) towfish and digital conversion unit run by a newly developed topside processing software package hosted on a Sun® workstation computer. The system has been developed by OIC during the past two years. The side-scan system is commercially available from EdgeTech® and the topside processing software is available for workstation computers from OIC.

Overall Assessment

Side-scan sonar does appear to be the most appropriate system for initial location of proud UXO prospects on the seabed. However, significant operational problems, discussed below, essentially prohibited a thorough examination of the capabilities of this system, though the system did produce apparently good data covering the entire test range. There is some question about the reliability of the particular hardware used, and future workers may get better results with other designs. Of the two data acquisition systems tested, the following conclusions are apparent:

1. The OIC workstation-based system has significantly better real-time observation capabilities and thus offers better opportunities for rapid target identification than the MMTC PC-based system.

2. The PC-based system is considerably more robust and easier to operate than the workstation system. The relative complexity and slow re-boot time of the workstation system (UNIX operating system vs. DOS) make it more difficult to transport and more time-consuming to implement.

Given the current rapid pace of developments in the simplification of workstations and the processing capacity of PC-based systems, it is likely that these conclusions will be moot in the near future.

The data analysis presented below suggests that, even with the limitations which existed in the survey, the system is capable of identifying about one third of the proud targets within range of the system. As would be expected, detection is easiest on flat, sandy surfaces and most difficult in areas with hard, irregular substrates. Surprisingly, there appears to be little correlation between the magnitude of the sonar return and the size of the targets, within the ranges explored in this study. No discrimination between UXO and metallic, non-UXO targets was achieved.

Primary Data Analysis

While the data were being collected, likely targets (i.e. small targets with high back-scatter) were selected from the incoming data stream by the workstation operator, and 250 x 250 pixel samples about these selected targets were recorded in separate files. A total of 211 such selections were made.

Data collections efforts were severely impacted by several mechanical and electronic failures. In addition, replacement components supplied by the manufacturer were ill-tuned and not field adjustable, resulting in degraded data quality for the 500-KHz data. Electrical grounding problems and acoustic noise from external sources impacted the 100-KHz data as well for some portions of the data.

OIC provided real-time integration of sonar data and navigation and post-acquisition playback processing for target identification and location. Due to these noise sources, not all data were sufficiently noise-free for sub-meter target detection, but the 8 data lines, processed and included in Folio Fold-out Map 2, cover the majority of the survey area. The data files from each line were processed by OIC, and a list of target prospects, with associated sonar images, were provided to MMTC for further examination. Significant problems discovered in data processing are detailed below.

1. **Poor Dynamic Range/System Gains.** As mentioned above, the internal system time-varying-gain (TVG) pre-sets were ill-set by the manufacturer, and not field adjustable with the tools available to us at the time. While the data range of the 500 KHz exceeded (and saturates) above 10 bits, that of the 100 KHz data does not even reach a full 8 bit dynamic range (see Figure 2). This saturation of the 500 and low dynamic range of the 100 KHz data severely limited our ability to detect targets.

2. **Noise Corruption and Poor System Beam-pattern.** OIC applied adaptive beam-pattern correction to the data, but undoubtedly some loss in signal/noise resulted because of the poor initial beam pattern in the system. While significant image area has been recovered by reduction of beam-pattern artifacts, random shot-noise and "tiger-striping" due to grounding fault severely impacted the data. More than half the data collected were corrupted by such noise. While efforts to reduce these problems will continue after this report, it is clear that the proper remedy is better control over data collection.

3. **Navigation.** After filtering of attitude, navigation and gain corrections, each "line" of data was digitally mosaicked, allowing superposition of known target locations on geo-referenced imagery to aid in detection of acoustic targets in the full-resolution data visible simultaneously in the waterfall. While numerous targets were detected in this fashion, we were unable to provide more than a "target/no-target" response, due to absence of auxiliary classification information.

4. **Lack of Towfish Heading:** Early in the surveying, the heading indicator on the towfish stopped working. As discussed below, this exacerbated the problems already present in the location of the target prospects.

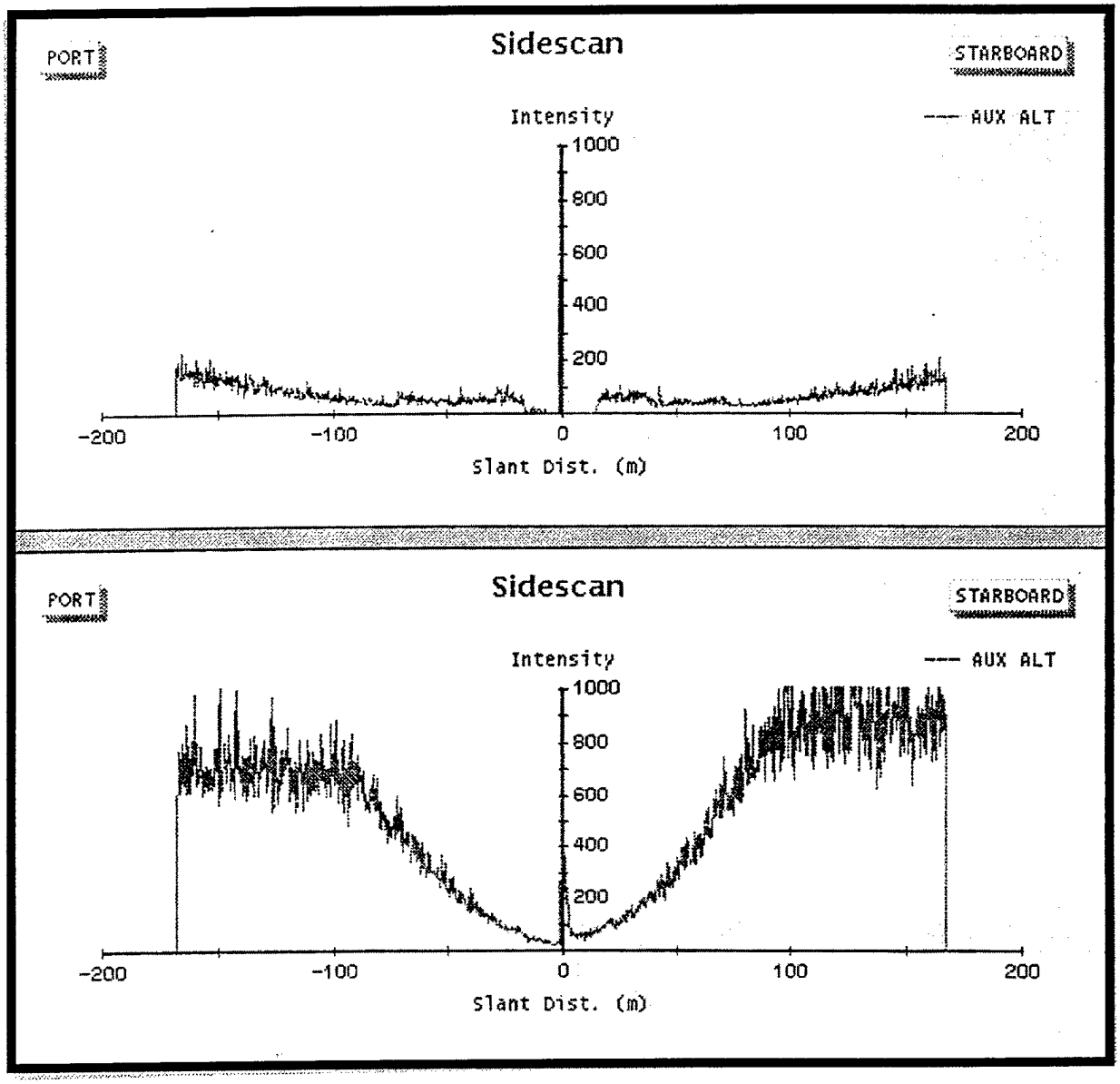

Figure 2. Screen Capture Showing Side-scan Signal Dynamic Range

Figure 3 shows the distribution of the side-scan sonar data, and the coverage of that data within the survey area. Nominal line spacing and range were 150 m, creating 100% overlap. A total of 6 survey lines were of sufficient quality for processing, including lines 4, 5, 6, 7, 9 and 10. The targets detected in each line or pair of lines are discussed below. Examination of overlapping swaths of sonar data in the side-scan sonar mosaic indicate that relative navigation is in good agreement track-to-track for lines 9, 7 and 6, with features matching to better than 10 meters (mosaic resolution is 0.5 meters). Lines 5 and 4, however, exhibit up to 50 meters of feature mismatch, indicating a break-down in navigation quality in deeper waters.

Secondary Data Analysis

In an attempt to address the primary objective of the project, efforts were made to resolve the clear discrepancies between the data collected by the side-scan system and the known locations of the proud targets. The following sections describe this effort. First, the assumptions and methodology are described, and then the results of the analysis are presented. Finally, the potential implications for using side-scan sonar to locate and classify UXO are discussed.

Assumptions and Methodology

Without some correction for the large errors made in navigation, it is not possible to perform direct comparisons between the known targets on the seabed and the resultant sonar images which are produced from them, since the mean distances between actual target positions are on the order of the position error. To provide such correction, the following assumptions are adopted:

1. The erroneous position assigned to at least one of the target prospects noted during each survey line lies relatively close (within 100 m) to the actual target position, and the actual target has the closest target location (of the known targets) to this erroneous position.

2. The error for each survey line is systematic and can at least be approximated by a single offset for the entire line. This assumption is justified if most of the navigation error is caused by wind and layback and currents. These offsets should be consistent during a single survey line, where speed and heading are maintained as constant as possible. Such offsets will move the towfish offline behind the survey vessel, leading to a lateral offset as well as a towfish heading error.

Based on these assumptions, the following algorithm was applied independently to each survey line to adjust the target prospect positions. All work was done on a desktop personal computer using the QBasic programming language.

1. The closest target for each prospect position is identified.

2. Using the position offsets from the larger (medium size and weight and larger targets) target-prospect pairs, the survey-line positions are sequentially adjusted for each offset.

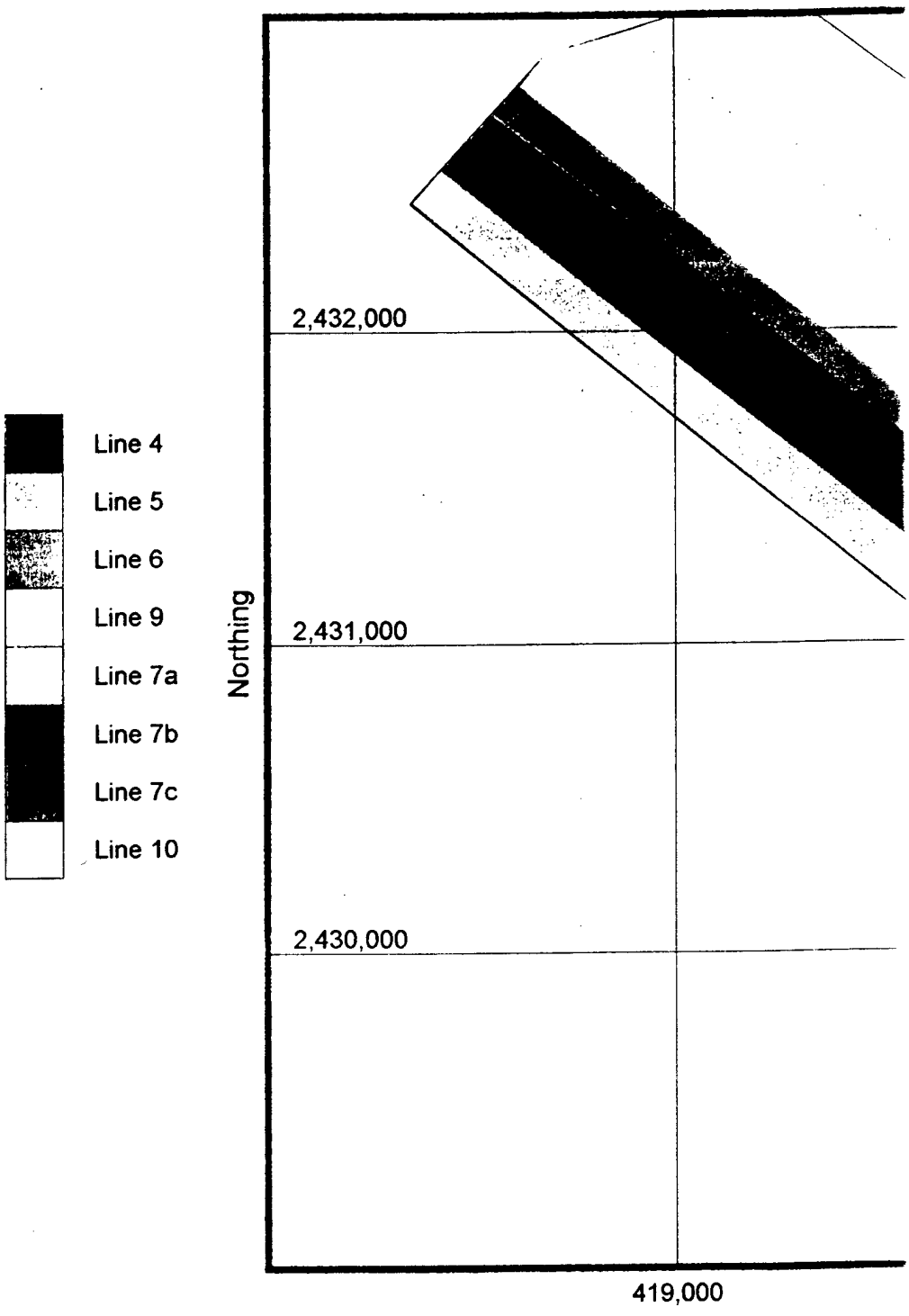

Figure 3. Approximate Distribution of

.te Distribution of Side-Scan Sonar Coverage

(2)

3. The offset resulting in the minimum sum of target-prospect distances is selected as the optimum adjustment of the survey line.

4. New positions are calculated for all prospects, and prospects which are less than 50 m from their associated targets are included as detected targets. Other prospects are deemed to be false positives.

Clearly, this adjustment must result in some improvement in correspondence between the prospects and targets, and such improvement by itself proves nothing. Thus another key part of this analysis is the identification of independent criteria to validate or refute the efficacy of the procedure. Three such criteria are examined here.

1. **Systematic Offsets Consistent With Ambient Conditions.** If the major navigation errors are due to current and wind sets or due to primary layback errors, then then the position offsets generated by this process should be physically meaningful within the context of the wind and tidal currents in the survey area or at least consistent during each survey line.

2. **Target Bias.** Presumably, targets with exposed angular surfaces are more likely to result in a significant sonar return than smooth ones. Random assignment of the targets with the prospects would produce the same frequency distribution of target size classes in the "detected" population as in the original target population. Real detection of targets should produce a distribution of target shapes which shows higher frequencies of the more angular classes than is present in the original population.

3. **Substrate Bias.** Targets on smooth, absorptive substrates such as sand are expected to be easier to detect than those on rough, hard substrates. Thus the distribution of detected targets should show a higher occurrence of targets on smooth, soft substrates than exists in the original target population.

Analytical Results

Table 1 presents the adjusted positions of the prospects and the identifications of the associated targets. Table 2 presents the summary data on the calculations of the offsets and the relevant tidal information for each run. Note that all but two of the runs indicate sets to the west of the side-scan towfish. This is consistent with the expected tidal currents (e.g. Gerritsen, 1978) and trade-wind activity during the surveys. Note also that all but one of the sets are less than 50 m, though the cut-off in the algorithm was 100 m. Improvements in the overall fit of the data to the actual target locations varies from 1% to 24%. The improvements are calculated using all the data, before the selection of targets less than 50 m from the associated prospect sonar returns.

In order to obtain some basis for error calculations related to detection rates, the data for each survey line were examined separately to estimate the variance to be expected in detection rate. Table 3 summarizes these data. The mean detection rate among the survey lines is 45.7%. This implies a coefficient of variation of 0.314. Using large sample statistics we can assume that the standard error of the estimate can be scaled as inversely proportional to the square-root of

Table 1. Side-Scan Target Detection Prospects

Survey Line	Prospect ID	Adjusted Easting	Adjusted Northing	Target ID	Nav. Error
4	54-01	420935.0	2430107.8	D006	20.6
4	54-03	420923.0	2430109.0	D006	9.6
4	54-04	420818.3	2430346.0	D022	30.7
4	54-05	420682.9	2430467.0	D026	42.9
4	54-06	420700.1	2430360.0	D020	49.1
4	54-08	420435.2	2430592.3	D035	25.4
4	54-11	420011.9	2431039.0	D068	37.4
4	54-19	419232.1	2431833.0	D126	27.7
4	54-20	418998.3	2432064.3	D146	34.2
4	54-21	418830.2	2432225.8	D158	0.0
4	54-22	418747.0	2432321.8	D164	31.8
5	54-26	419065.9	2431972.8	D138	15.9
5	54-29	419319.1	2431667.8	D119	12.2
5	54-32	420045.3	2431098.8	D068	35.2
5	54-34	420440.6	2430575.8	D035	37c
5	54-36	420516.2	2430402.0	D025	28.8
5	54-37	420746.4	2430463.0	D026	44.0
5	54-38	420746.7	2430344.5	D020	0.0
5	54-42	421218.5	2429807c	C035	39.5
5	54-43	421252.3	2429791.0	C023	47.4
6	69-00	420721.8	2430462.5	D026	28.7
6	69-01	419886.1	2431518.8	D105	48.3
6	69-09	419205.2	2432087.0	D149	20.7
6	69-62	421408.5	2429913.5	C021	39.3
6	69-64	421425.5	2429987.0	C020	21.5
6	69-65	421373.9	2429932.3	C021	0.0
6	69-66	421300.2	2430072.5	C032	40.3
6	69-67	421261.6	2430206.5	D013	27.7
6	69-68	421172.0	2430014.0	C045	33.6
6	69-70	421041.9	2430083.0	D004	26.4
6	69-74	420722.1	2430463.0	D026	29.3
7a	7A-00	421449.5	2429863.0	C009	3.9
7a	7A-03	421399.3	2430023.0	C020	23.1
7a	7A-04	421349.7	2429936.5	C021	24.6
7a	7A-05	421280.6	2429968.5	C033	0.0
7a	7A-07	421315.4	2430055.3	C032	20.6
7a	7a-10	421016.3	2430517c	C056	26.8
7a	7a-11	420947.4	2430468.5	D029	4.0
7a	7a-13	420811.2	2430606.8	D034	7.0
7a	7a-15	420458.9	2430729.3	D047	34.2
7b	7B-00	421449.6	2429863.3	C009	3.6

Table 1. Page 2/3					
Survey Line	Prospect ID	Adjusted Easting	Adjusted Northing	Target ID	Nav. Error
7b	7B-01	421355.2	2429932.0	C021	18.7
7b	7B-04	421475.7	2429957.5	C008	31.1
7b	7B-06	421280.6	2429968.5	C033	0.0
7b	7B-02	421399.5	2430023.5	C020	23.4
7b	7B-07	421315.1	2430054.8	C032	20.9
7b	7B-05	421483.3	2430081.5	C019	7.4
7b	7B-08	421354.2	2430147c	C031	36.1
7b	7B-09	421081.5	2430169.3	D010	6.1
7b	7b-13	421014.5	2430518.5	C056	29.0
7b	7b-15	420845.2	2430594.5	D034	30.8
7c	7C-01	420678.9	2430892.3	D059	46.8
7c	7C-02	420464.3	2430741.5	D047	32.9
7c	7C-03	420502.9	2430756.5	D048	19.8
7c	7C-05	420373.9	2430866.0	D057	42.1
7c	7C-06	420504.7	2430960.8	D060	41.4
7c	7c-17	419741.9	2431549.5	D107	19.6
7c	7c-19	419375.1	2431952.0	D134	39.2
7c	7c-20	419314.5	2432174.0	D155	16.0
7c	7c-21	419228.1	2432108.8	D149	30.0
7c	7c-22	419198.2	2432106.5	D149	0.0
9	69-21	419189.5	2432350.0	D172	39.3
9	69-23	419378.6	2432371.5	D171	22.1
9	69-25	419457.7	2432244.5	D160	15.9
9	69-29	419601.2	2432005.5	D141	20.4
9	69-34	419973.1	2431713.5	D122	44.8
9	69-35	420121.1	2431573.8	D109	24.0
9	69-36	420171.5	2431591.8	D109	47.7
9	69-38	420253.1	2431500.0	D106	29.2
9	69-40	420411.5	2431319.5	D092	34.5
9	69-46	420943.2	2430678.3	D039	22.7
9	69-48	421164.5	2430501.0	C053	14.0
9	69-50	421055.6	2430506.0	C056	23.5
9	69-51	421100.8	2430576.3	C055	9.8
9	69-52	421191.2	2430385.8	C052	29.9
9	69-53	421238.7	2430451.5	C051	19.4
9	69-54	421252.0	2430304.5	C050	6.7
9	69-55	421320.5	2430350.5	C049	20.3
9	69-57	421406.5	2430355.0	C041	7b
9	69-59	421381.7	2430154.5	C031	13.6
9	69-60	421610.0	2430122.3	C006	4.5
9	69-61	421560.4	2430028.8	C007	0.0
9	69-63	421370.4	2429806.0	C010	38.3

Table 1. Page 3/3					
Survey Line	Prospect ID	Adjusted Easting	Adjusted Northing	Target ID	Nav. Error
9	69-69	421130.0	2430191.3	D010	47b
10	10-02	419844.7	2431908.3	D131	12.6
10	10-03	419755.4	2432030.0	D143	47.8
10	10-08	419228.5	2432522.5	D180	18.8
10	10-09	419181.4	2432684.5	D189	39.6
10	10-14	419767.9	2432433	D177	31.8
10	10-16	419878.4	2432272	D163	0
10	10-19	420204.8	2431957.5	D137	23
10	10-21	420382.6	2431948.8	D139	32.5

Table 2. Effects of Adjusting Survey Lines and Relevant Tidal Data

Survey Line	4	5	6	7a	7b	7c	9	10
%Gain*	5	22	1	19	24	3	2	3
dx(meters)	-33.0	32.1	9.8	6.5	6.6	11.1	-8.4	13.6
dy(meters)	4.0	60.8	2.8	-25.8	-25.5	-13.0	7.5	-7.5
Start Time	14:08	13:18	13:05	09:24			14:14	09:24
Finish	14:48	13:57	13:58	10:19			14:46	10:19
High Tide	09:50	09:50	08:40	08:40			08:40	8:40
Low Tide	17:30	17:30	15:00	15:00			15:00	15:00
Tidal Stage	ebb	ebb	ebb	ebb			final ebb	high stand
Line Direction	S	N	S	N			N	N

*Percent decrease in mean distance between prospects and associated targets after adjustment

Table 3. Target Detection Rates

Survey Line	Available Targets*	Number Detected	Percent Detected	Area Covered (km^2)
4	36	11	31	0.635
5	27	9	33	0.682
6	39	11	28	0.761
7a	19	9	47	0.268
7b	15	11	73	0.191
7c	23	10	43	0.545
9	39	23	59	0.781
10	16	8	50	0.322

*All proud targets within 100 m horizontally off the vessel track

Table 4. False Positive Side-Scan Detection Prospects

Survey Line	Number of Prospects	Number With Associated Targets	Percent False Positives
4	21	11	48
5	20	9	55
6	27	11	59
7a	15	9	40
7b	16	11	31
7c	25	10	60
9	40	23	43
10	17	8	53

To investigate the role that the substrate may have in influencing the resultant detection rate, we use the substrate types noted for each target by NFESC. We summarize these as follows:

1. Smooth sand

2. Sand with ripples

3. Sand with sand waves

4. Sand with rubble (with or without limu, soft algae)

5. Hard, flat rock

6. Irregular rock and a cave

Table 5 summarizes the detection rates for these various categories. Duplicate detections, which occured commonly because of the extensive overlap between runs, are not counted in this analysis. As can be seen in this table, there does appear to be some difference in detection rate among the substrate types, particularly if the first three and last three categories are lumped into two larger groups.

Table 5. Effect of Substrate on Target Detection

Substrate	Available Targets	Targets Detected	Percent Detected	Estimated Error (%)
1	43	14	33	7
2	52	26	50	8
3	6	2	33	16
4	72	23	32	5
5	3	2	67	77
6	3	1	33	51
1,2&3	101	42	42	6
4,5&6	78	26	33	5

To investigate the potential effect of target types on the detection rate, we initially grouped the targets by size and weight, similar to the categories adopted by NFESC in their description of the targets. This exercise does not show any increase in the percentage of larger targets in the set of detected prospects, and the Pearson correlation coefficient calculated between size class and prospect detection strength, as defined in our preliminary report to NFESC, is 0.06. After some discussion with various colleagues on this matter, we formulated another set of classes, based on shape rather than size. An acoustic echo should be stronger from exposed, angular surfaces than
from smooth round surfaces. On this basis we organized the targets into four classes: Class 1, which includes round cylindrical shapes with relatively low elevation when lying on their sides, Class 2, which includes slightly higher profiles and some flat surfaces exposed, such as oil drums, Class 3, with sharp angular edges but horizontal, low profiles, such as ammo boxes, and Class 4, with significant exposed, angular surfaces at relatively high profiles, such as bombs and projectiles with fins. The classes for the detected targets are shown in Table 6. The correlation between these categories and the sonar reflection strengths (termed "prospect return class" in the table) is almost as bad as the size classes (r=0.07). The apparent bias of the detected targets for the higher classes, presented in Table 7, is intriguing, though not compelling.

Table 6. Shape Classifications of Detected Targets

Target ID	Target Description	Target Shape Class	Num. Prospect Hits	Prospect Return Class
C006	MK81	1	1	2.0
C007	MK81	1	1	3.0
C008	FRAG	1	1	2.0
C009	MK82	1	2	2.0
C010	MK81	1	1	3.0
C019	3MK106	4	1	3.0
C020	MK76	4	3	2.7
C021	MK76	4	4	2.0
C023	MK76	4	1	2.0
C031	PROJ554	1	2	2.5
C032	PROJ538	1	3	2.3
C033	PROJ538	1	2	2.0
C035	PROJ554	1	1	2.0
C041	ROCK5	1	1	3.0
C045	ROCK5	1	1	3.0
C049	ROCK275	4	1	2.0
C050	CART20M	3	1	3.0
C051	CART554	3	1	3.0
C052	CASE40M	3	1	3.0
C053	MKI06	4	1	3.0
C055	ROCK7	4	1	3.0
C056	2ROCK275	4	3	1.3
D004	LDRUM N/A	2	1	3.0
D006	MDRUM N/A	2	2	1.0
D010	AM_BOX N/A	3	2	2.0
D013	MK76 Practice Bomb	4	1	3.0
D020	5APIPE N/A	1	2	2.5
D022	3SPIPE N/A	1	1	2.0
D025	CART20M Other	3	1	1.0
D026	AM_BOX N/A	3	4	2.0
D029	ROCK5 RocketWhd	1	1	2.0
D034	ROCK275RocketWhd	4	2	2.0
D035	ROCK7 RocketWhd	4	2	2.0
D039	MK106 PracBomb	4	1	3.0
D047	2PROJ538Projectile	1	2	2.0
D048	MK106 PracBomb	4	1	3.0
D057	ROCK5 RocketWhd	1	1	3.0
D059	CART20M Other	3	1	2.0
D060	MK76 Practice Bomb	4	1	3.0
D068	PROJ554Projectile	1	2	2.0

Table 6. Page 2/2				
Target ID	Target Description	Target Shape Class	Num. Prospect Hits	Prospect Return Class
D092	CART762 Other	3	1	1.0
D105	LCHAIN N/A	4	1	2.0
D106	CART554 Other	3	1	2.0
D107	MK106 PracBomb	4	1	3.0
D109	ROCK7 RocketWhd	4	2	2.5
D119	ROCK275RocketWhd	4	1	2.0
D122	2MK76 PracBomb	4	1	3.0
D126	MK76 Practice Bomb	4	1	2.0
D131	CASE40M Other	3	1	3.0
D134	ROCK7 RocketWhd	4	1	3.0
D137	2ROCK5 RocketWhd	1	1	3.0
D138	ROCK5 RocketWhd	1	1	2.0
D139	4SPIPE N/A	1	1	3.0
D141	MK82 Large Bomb	1	1	2.0
D143	ROCK275RocketWhd	4	1	3.0
D146	ROCK7 RocketWhd	4	1	2.0
D149	3MK106 PracBomb	4	3	2.3
D155	MK106 PracBomb	4	1	3.0
D158	MK81 Large Bomb	1	1	3.0
D160	MK81 Large Bomb	1	1	2.0
D163	MK76 Practice Bomb	4	1	3.0
D164	4SPIPE N/A	1	1	2.0
D171	ROCK275RocketWhd	4	1	2.0
D172	AM_BOX N/A	3	1	2.0
D177	ROCK275RocketWhd	4	1	3.0
D180	PROJ554Projectile	1	1	2.0
D189	ROCK275RocketWhd	4	1	1.0

Table 7. Differences in Target Detection and Target Shapes

Shape Class	Available Targets	Number Detected	Percent Detected	Estimated Error
1	71	25	35	6
2	7	2	29	14
3	29	11	38	9
4	72	29	40	6
1&2	78	27	35	3
3&4	101	40	40	3

Potential Implications for UXO Location and Classification

As discussed above and in the Observational Notes below, the system used in this demonstration, because of navigational and other constraints, was by no means optimized for the job. However, in spite of these problems, the data do suggest that the technique in general has significant potential. The adjustment of survey line locations was in general consistent with a set of the towfish by wind and tidal currents, but did not result in dramatic improvement of the correspondence between the prospect and target positions. Adequate navigation for this purpose must have better control over the relative towfish position with respect to the survey vessel than was possible in this survey. Overall, the system appears to be able to detect approximately 40% of the targets on smooth, sandy areas, and much lower percentages of the targets in hard, irregular areas. There is an apparent false-positive detection rate of about 50%.

The statistics indicate marginal discrimination between the detection rates for different target shapes, and no distinction by target size. The survey data show consistency of the trends observed in the substrate and target bias estimates with expectations based on theoretical considerations, though the magnitudes of these trends are statistically marginal.

We suspect that the detection rates provided here are a good first approximation, and that much improvement is possible with respect to location precision, reduction of false positives, and shape discrimination. We believe it unlikely that the tool by itself will be capable of discerning UXO from non-UXO objects. Based on the complete lack of correlation noted between the prospect return signal strength and the actual target size, it is probable that other tools will be necessary complements to constitute an effective search technology.

Operational Notes

1. Operator errors (improper sealing of the towfish electronics) led to significant damage to the DF-1000 towfish. MMTC had tried to obtain a complete set of spares for the system, but they were unavailable from the manufacturer more than four months prior to the operation. We did manage to get a working system by borrowing the manufacturer's only functioning lab-test system and did complete the required surveys, but only at the end of the survey period. The lack of accurate navigation for the towfish, as described above, exacerbated the problem and has made simple interpretation of the records impossible.

2. Time-varying gain (TVG) is set by processors within the towfish which cannot be adjusted in the field. The unit provided by the manufacturer had a TVG for the 500 kHz signal which was misadjusted so that this data channel was clipped severely; only the near-field (<20 m lateral on the seabed) data are usable. This is a significant design problem for the DF-1000. The TVG should be adjustable in the field.

3. The DF-1000 is extremely sensitive to the properties of the signal cable, and accidents due to unexpected stress on the wire, mishandling, or other incidents leading to shorts or an open circuit can easily do major damage to the towfish electronics. Though this was not a factor in these operations, it is important to note in the evaluation of the system.

AAHIS SYSTEM

System Description

Because this system is not commercially available except from SETS Technology, Inc. it is described in somewhat more detail than the other, more conventional systems. AAHIS, the Advanced Airborne Hyperspectral Imaging System, has been developed by SETS Technology, Inc. SETS Technology, Inc. has developed a flight-tested, visible/near-infrared (432 nm to 830 nm) hyperspectral imaging system, optimized for use in maritime and near-shore applications. AAHIS is the technique of imaging a scene in many (tens or hundreds) of color bands, so that a complete spectrum is recorded at each spatial location in the image. Hyperspectral imaging (HSI) is distinguished from multispectral imaging by the number of spectral bands recorded (multi-spectral imagers typically record no more than a dozen spectral bands); by the narrowness of each hyperspectral band (typically 10 nm wide or less); and by the contiguous nature of the hyperspectral data. Hyperspectral imaging is distinguished from point spectrometry by the collection of spectral data sets for complete images, instead of just one point at a time.

System Concept

The AAHIS sensor is a "pushbroom" type imager which builds the image line-by-line. The sensor's primary optic images the scene onto the entrance slit of the spectrometer, so that only light from a single narrow image line (i.e., the pushbroom), oriented perpendicular to the direction of motion of the sensor, is allowed to pass into the spectrometer. Inside the spectrometer, this polychromatic line image is simultaneously dispersed into a two-dimensional spectrum and re-imaged onto the focal plane array. As the aircraft moves forward over the scene, the image of the slit scans the terrain below and the strip image is built up line-by-line, producing a hyperspectral "data cube" consisting of a stack of up to 288 monochromatic images. Spectral information is collected simultaneously in each of 288 separate bands of approximately 1.4 nm/band. In order to match spectrometer aberration and reduce data rate, the spectral dimension is nominally binned on the chip by 4, giving a spectral bandwidth of 5.5 nm.

Spatial resolution is determined by the sensor's instantaneous field of view (IFOV), by the spectrometer aberration, and by the frame L rate/ground speed of the aircraft. At an altitude of 1 km, with a frame rate of 40 frames per second and a ground speed of 80 knots (typical values), the ground sample distance (GSD) is approximately 1 m, which corresponds to the angular width of two pixels on the focal plane array. Therefore, to match the same GSD across-track as along-track, the chip is nominally binned by two in the spatial direction. This yields 192 spatially resolved channels. At this frame rate and for the 2x4 on-chip binning, the data is being recorded at 1.1 MB/sec. This is well within the data system recording capability (i.e., SCSI II interface capability).

Sensor Components

The AAHIS sensor (see the block diagram below) consists of the following: the imaging spectrometer (including the primary optics, or "foreoptics"); the spectrometer focal plane array

and controller; a scene monitor camera with video monitor and SVHS videotape recorder; a timebase generator; a computer with hard disk and 5 GB tape drive; the spectrometer vibration isolation mount and rack structure to mount the above items in the aircraft cabin (mounted to the seat rails); and an AC inverter power supply.

The low aberration, high throughput, and wide-field performance of the AAHIS imaging spectrometer are the key elements that enable the level of demonstrated capabilities. Light enters the f/4, 50 mm focal length foreoptic and is imaged onto the slit of the spectrometer. Light through the slit passes through a two-element field flattening lens onto a single plane reflection grating. A second reflective element images (with magnification less than one) onto the spectrometer focal plane array (FPA). The FPA is a high speed frame-transfer CCD with 385x576 pixels cooled to less than -20 °C. This FPA incorporates a UV-enhanced coating which increases the silicon CCD quantum efficiency for wavelengths shorter than 450 nm. The FPA uses "frame transfer" readout, wherein photocharge in the active, exposed central half of the FPA is quickly shifted under a mask to be read off the chip while photocharge from the next frame is integrated in the active half [i.e., the active portion of the FPA is 385 (spatial) x 288 (spectral)]. This reduces the read rate of the chip (i.e., electronic noise) and minimizes spectral/spatial "smear" during the readout of the FPA (i.e., 1.2 ms frame transfer compared to an approximate 25 ms integration time). Photocharge from each pixel is transferred to the gate of an FET, where it is converted into a voltage signal. This analog voltage signal is then converted into a 12-bit number by an analog-to-digital converter. Two 8-bit bytes are used to store the value of each pixel to prevent distortion of the upper or lower bit.

Computer Control

The AAHIS sensor is controlled by a Macintosh Quadra 800 computer, equipped with 72 MB of RAM. During data collects, image data are written directly to this RAM, so that approximately 2400 frames (60 seconds of data at 40 frames per second) may be collected in an uninterrupted sequence before data must be transferred to a disk file on the Quadra's 1.2 GB internal hard drive (this takes approximately 10 seconds). Raw data may be downloaded to the 5.0 GB Exabyte tape drive between aircraft data runs.

A standard color CCD "spotter" camera supplies a video signal to a small monitor allowing the operator to view, in real time, the same ground scene the sensor is seeing. The scene is also ~captured by an SVHS videocassette recorder. A timebase is recorded directly onto the SVHS tape by a time code generator.

The spectrometer is cradled in a welded, black anodized aluminum frame on four vibration isolation mounts. The electronics (computer, camera controller, tape drive, time code generator and videocassette recorder) are mounted in a separate anodized, welded aluminum frame. Both frames are locked to the aircraft's seat rails. This permits rapid installation of the system in the aircraft. The sensor and scene monitor camera, having been precisely boresighted, look down through a windowless hole in the aircraft floor.

Image Processing

Processing is accomplished with HIPS™ SETS Technology's proprietary Hyperspectral Image Processing System. A Sun/UNIX workstation-based package, HIPS is a full-featured spectral image processing system with unique capabilities for processing hyperspectral data sets. HIPS is now being ported to the Maui High Performance Computing Center (MHPCC). At the termination of a data gathering flight, a tape cartridge containing raw HSI data is produced, ready for flat and dark field corrections, HSI analysis, display and printing. In addition, an SVHS videotape of the spotter camera's record of the ground track is produced, allowing the data analyst to correlate the "normal" view of the scene with the hyperspectral imagery.

Overall Assessment

Based on discussions with SETS Technology personnel it is probable that this system in its present configuration is not effective in location and classification of most of the targets. As discussed below, operational problems do limit somewhat the confidence of this assessment and modifications to the system could have significant impacts on the system's effectiveness for this purpose.

Data Analysis

SETS Technology, Inc. collected ~5GB of raw data, calibrated and converted it into HIPS data file format for analysis. Intensive processing using various techniques has not, to date, revealed any obvious underwater targets. Sub-pixel beach targets were easily identified. All targets were subpixel in size which is the reason we feel we were unable to identify the underwater targets. Ground resolution varied according to aircraft altitude.

SETS Technology, Inc. developed a GIS system in ArcView to display the location of the calibration area ordnance along with the aircraft overflight data based on the Flight Navigation System (FNS) operated with AAHIS. This GIS was critical in determining, with any degree of accuracy, the known location of targets which allowed us to constrain our data processing efforts on such a large amount of total data to specific areas. We chose to concentrate on data from a few overpasses on 6 August, during which there were favorable cloud conditions and on data from shallow water depths (< 15 m). Figure 4 shows prints from ArcView indicating the flight paths over the calibration area for all of the flights on 6 August. Figure 5 shows prints from just flight 12 and 13.

Figures 6 and 7 show passes 1-30 for 6 August. The presence of clouds on 19-30 is clearly observable. We therefore processed the data for passes 12 & 13 for better cloud conditions, but also extensively processed pass 21 & 22. Figures 8 and 9 show spotter camera video data, RGB composite data, band 5 (blue), binned blue - binned red data, binned green - binned red data, and a ratio of the binned blue - red to binned green - red data for both scene 12 and 13. The effect of this type of processing was to subtract out the surface of the water to show more of just the underlying substrate (sea-bottom) conditions.

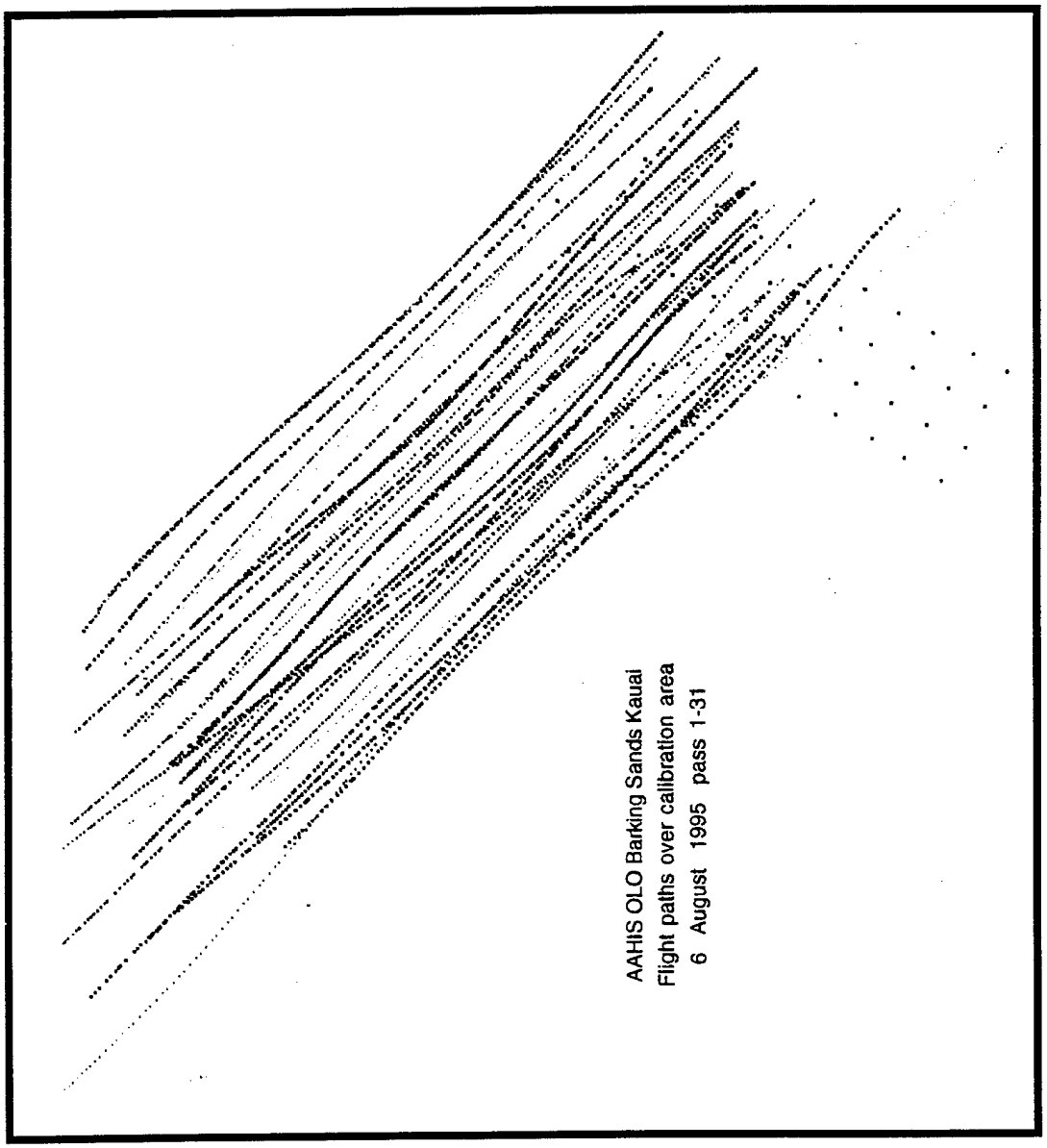

Figure 4. AAHIS Flight Paths over Calibration Area, 6 August, 1995

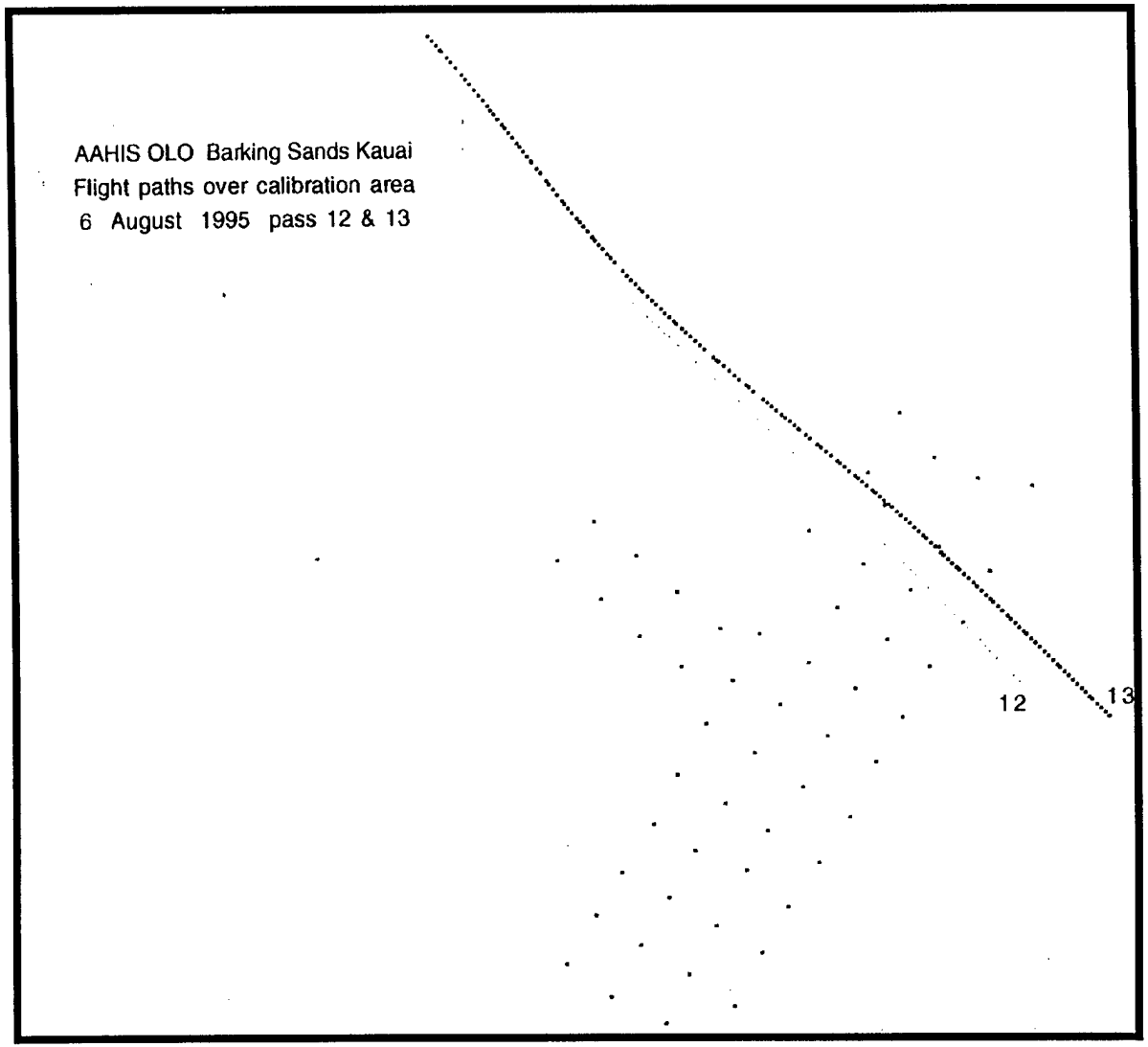

Figure 5. AAHIS Flight Paths 12 and 13, 6 August, 1995

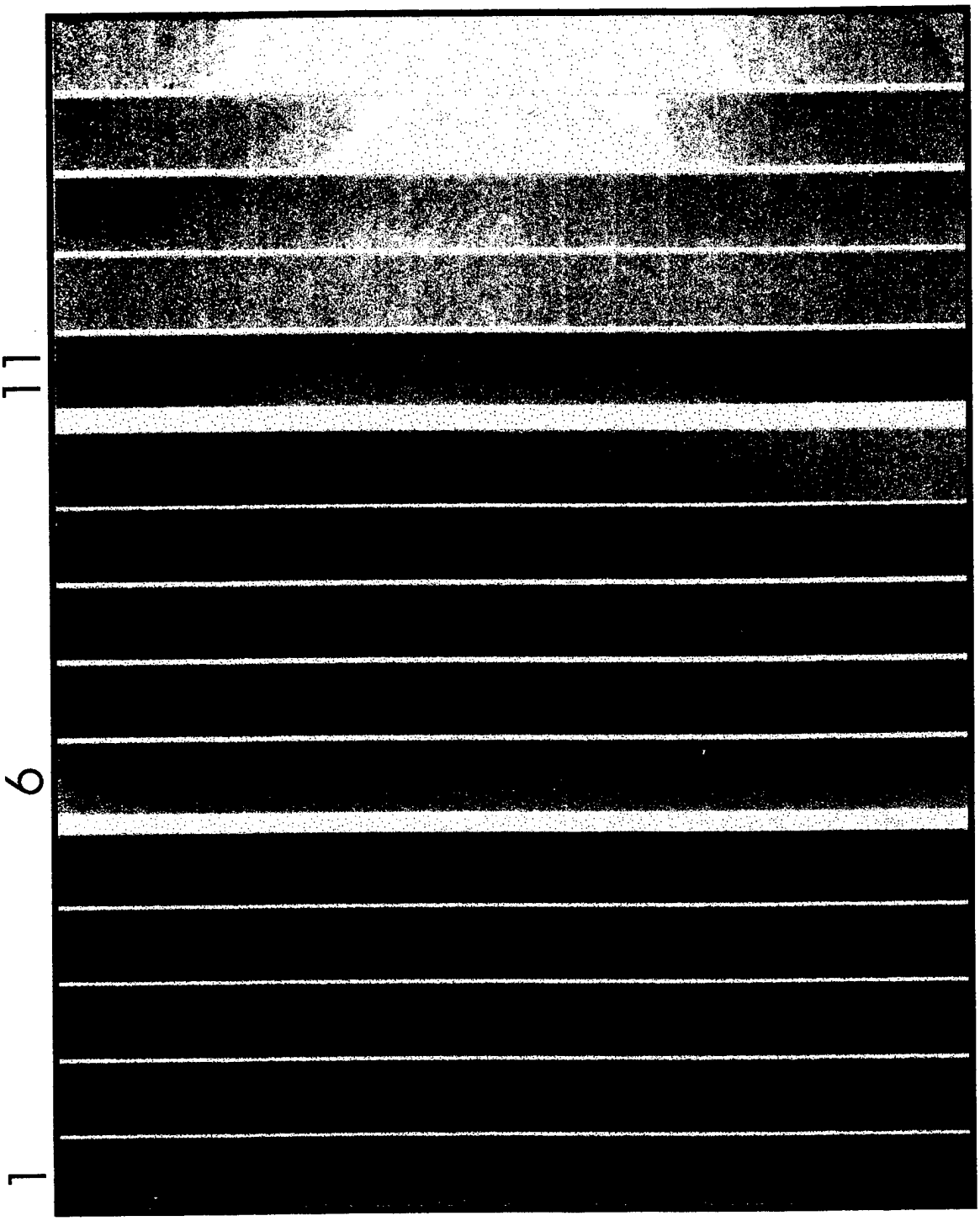

Figure 6. AAHIS Passes Over Test Range, 6 August, 1995 (1-15)

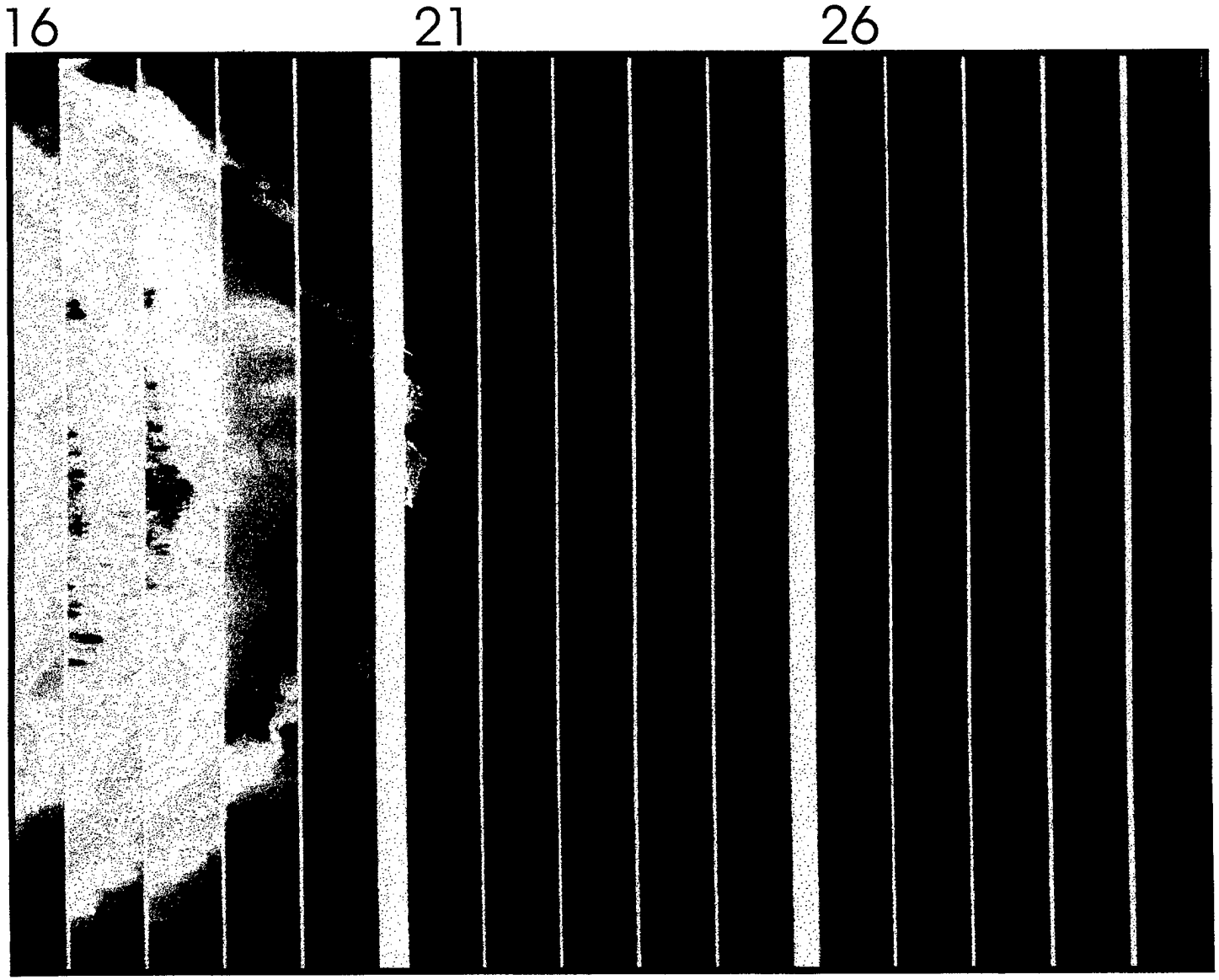

Figure 7. AAHIS Passes Over Test Range, 6 August, 1995 (16-30)

Figure 8. AAHIS Pass 12, 6 August, 1995 Color Isolation Analysis

Figure 9. AAHIS Pass 13, 6 August, 1995 Color Isolation Analysis

The targets located on the beach were identified. These include our calibration panels, a sub-pixel land mine, a 25 x 7" practice bomb, and a 11 x 3" rocket warhead. Ground photos of these targets are shown in Figure 10. Figure 11 shows both spotter camera and AAHIS data collections of these beach targets on 5 August (our calibration panels were subsequently stolen before the 6 August data could be collected). Principle Component Analysis (PCA) for two overpasses of the beach targets near the calibration panels revealed all 3 of the sub-pixel targets. The bottom three images in Figure 11 show the presence of a vehicle in the calibration area as the data were collected (probably driven by the people responsible for the theft of the calibration panels later that day).

Beach targets on 6 August were identified with PCA and are shown in Figure 12. Here we see the presence of a vehicle (known) and the hood of a car (used as a reference on the beach during the test) with a sub-pixel mine deployed above it and 2 sub-pixel targets located below. All three are visible in the PCA image in Figure 12.

Operational Notes

Twenty-six aerial passes over the range were made on 5 August. The presence of significant cloud cover and relatively high winds produced mostly shadowed data with significant sea surface turbulence. This resulted in relatively poor data quality. Thirty-three passes were made on 6 August. There was less cloud cover and lower winds, allowing significantly improved data quality. Some problems encountered during the data collection include the following:

- We encountered inclement weather on 5 August.
- We could not fly the North part of the area on 6 August due to it being a restricted missile launch area.
- All of the targets were extremely sub-pixel (< 20 % pixel size). Larger objects (with dimensions greater than about 2 m) deployed in the shallow water area would have made the processing much more robust. This lack of larger sized objects made it difficult to calibrate the processing and procedures of the AAHIS data in the shallow water search area.
- Underwater reference calibration targets were not deployed.
- Our surface calibration panels (deployed on the beach) were stolen from the deployment site during the 5 August data collection.
- Due to airspace restrictions placed by the Pacific Missile Range Facility on the airplane collecting the data, it was not possible to get good data from the northern half of the range.
- Due to the theft of a calibration panel placed on the beach before the overflight occurred, data processing options for the collection were significantly limited.

To date, the highest spatial resolution possible is limited chiefly by the turbulence-induced motions of the aircraft. These effects are mitigated somewhat by an inertial navigation system

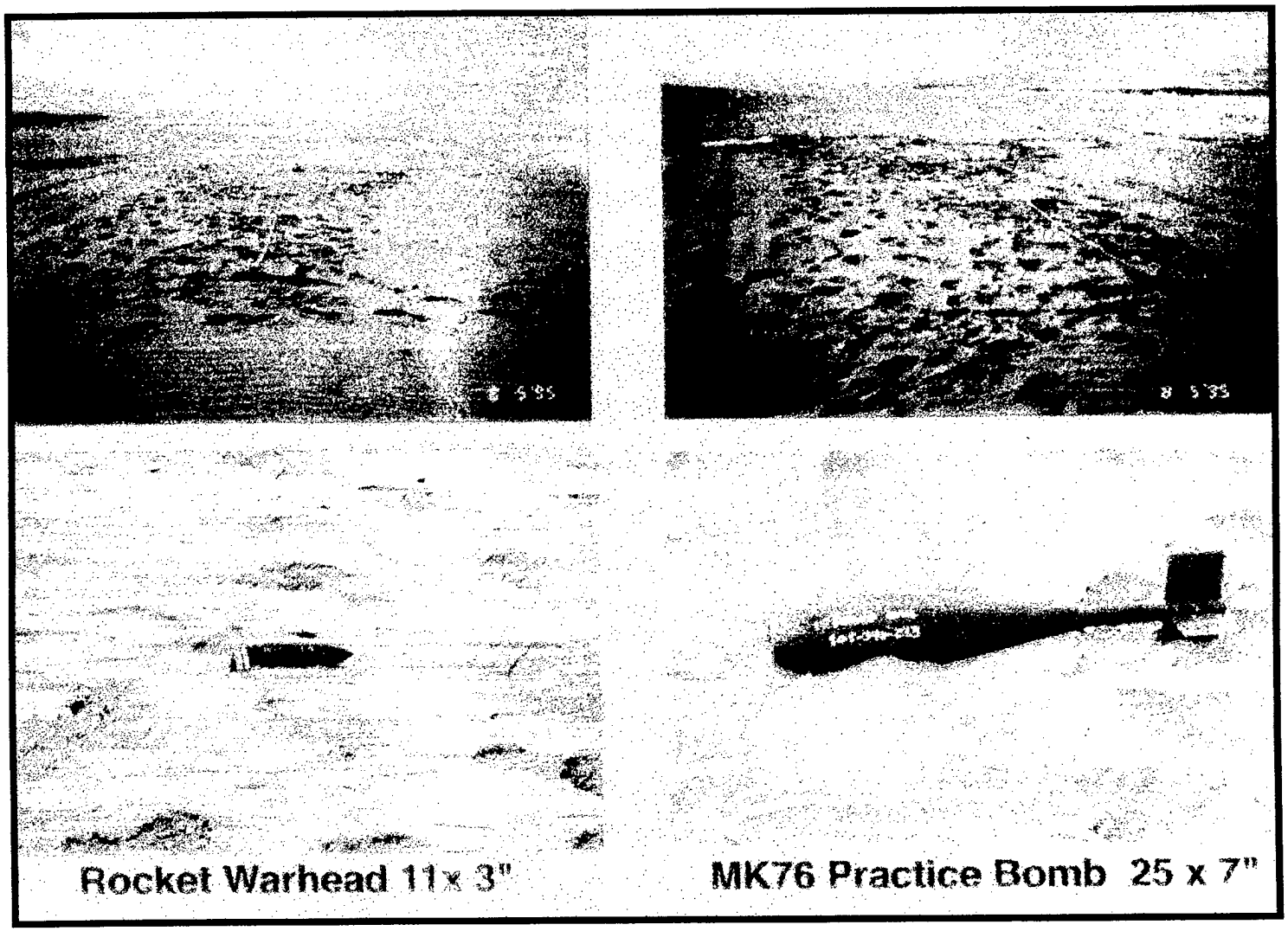

Figure 10. Beach Targets, 6 August, 1995

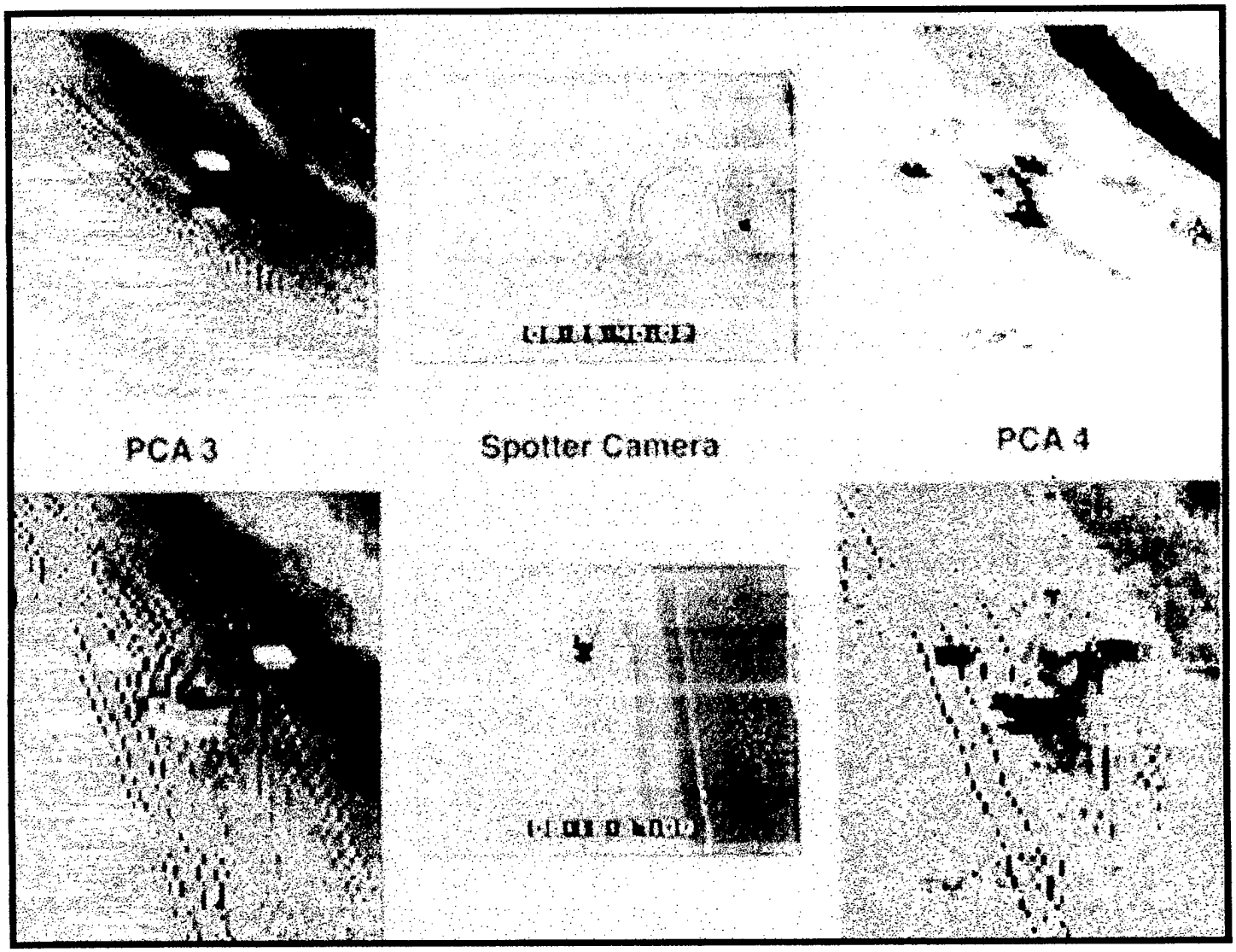

Figure 11. AAHIS Images of Beach Targets, 6 August, 1995

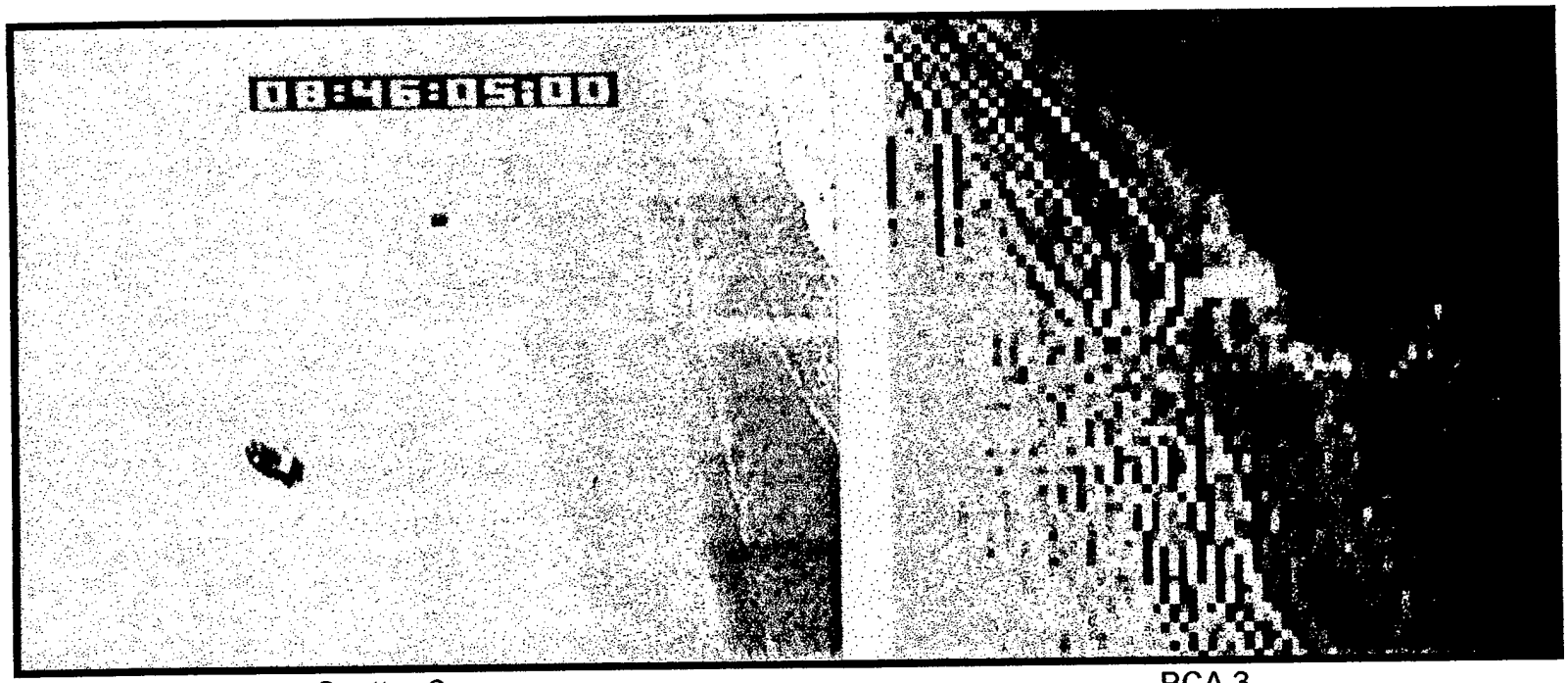

Figure 12. Beach Targets and Car Hood, AAHIS, 6 August, 1995

in the aircraft, but the ultimate pixel size is presently still limited to approximately 1 m. Targets which are significantly smaller than this size can be detected when their contrast with the ambient spectral pattern is sufficiently strong to produce a significant difference between the overall spectral pattern for the pixel in which they lie and its neighbors. The threshold for such detection can be lowered somewhat if the spectral characteristics of the targets are known. The AAHIS system was successful in detecting the sub-pixel sized targets placed on the beach, because they met these criteria. The reduced spectral variability caused by sea-surface reflections and light scattering by the seawater itself, however, left insufficient contrast for confident detection of the known seabed targets. If AAHIS can improve the spatial resolution, probably through improvements in the stability of the scanner or corrections for aircraft motions, its potential for ordnance location and classification would be greatly enhanced.

TIME-DOMAIN EM PULSE SENSOR

System Description

The system selected for use in this project is the J.W. Fishers Mfg., Inc. Pulse 12 Time-Domain Electromagnetic Detector. This sensor is capable of detecting both ferrous and non-ferrous metals on the surface and buried less than 0.5 m. It has been extensively field tested and used by many salvage and treasure hunting operations. The system selected for use here comes an altimeter for keeping the towfish a set distance off the sea floor. This system can detect non-ferrous, but conducting objects, such as brass or other non-magnetic metals. It has a range slightly less than the magnetometer but is essential since it is quite likely that many of the targets will be non-magnetic.

Overall Assessment

This tool was planned for use as a classification device for targets located by the other systems. However, initial testing of the sensor showed that it does not provide reproducible results which can be used for this purpose.

Data Analysis

No further data analysis is planned for this system.

Operational Note

The system was tested in conjunction with a Smithsonian Institution investigation of a ship wreck off the northern coast of Kaua'i. Anomalies detected with a standard proton precession magnetometer were investigated using the EM sensor, and good correlation was noted. Very small anomalies found with the magnetometer were very significant for the EM sensor, while large, probably bed-rock induced anomalies were not detected. However, when the EM sensor produced a significant signal, its baseline value shifted markedly, and it was not possible to repeat readings with any reproducibility. The tool might be useful in the future if a stable baseline can be achieved.

CHIRP SHALLOW REFLECTION PROFILER

System Description

During the past five years frequency modulated (i.e., "chirp") acoustic systems have undergone extensive development and are available commercially. This particular system was developed specifically for high resolution profiling of carbonate sand bodies by Lester LeBlanc and Steven Schock, the original developers of chirp acoustic instrumentation. It has a lower frequency band than the other commercially developed systems (about 500 - 1,500 Hz) and is available for local lease from the Oahu based firm Sea Engineering, Inc. It is field tested and confirmed effective in carbonate sands in Hawai`i for high resolution, shallow profiling to depths of at least 50 m. It is a prototype system, so cannot be said to be commercially available.

Overall Assessment

Because the system by itself can retrieve data only from a very narrow swath (< 3 m) directly beneath the towfish, its application for practical ordnance location and classification depends upon the array of receivers deployed by MMTC/CSD and discussed below. The system does provide an excellent real-time characterization of the seabed type, however, which was very useful in this project for confirming the soft-substrate types identified by the SeaBat® back-scatter records.

Data Analysis

No analysis of the data retrieved directly by the chirp transducers is planned. Comparison of the system with the GeoPulse® as an appropriate sound source is described below.

Operational Note

The Sea Engineering system proved to be a very well designed and robust system. Its only negative attribute is the size and weight of the towfish (~4' X 5' X 3'; 800 lb. in air) , which make deployment and recovery much more difficult than other systems and require special handling for shipment.

SEISMIC PROFILING

System Description

This system, developed and tested by MMTC/CSD, is basically a cross between a high resolution shallow profiling system and a reduced-scale 3-D oil-field seismic system. It is composed completely of components which are commercially available. An ORE Geopulse® sound source is used to generate an impulse with a spectrum between 500 to 2,500 Hz within 3 db of maximum output. It can be triggered at 0.25 second intervals to provide seabed and

sub-surface resolutions of approximately 0.5 m. It penetrates the seabed and retrieves useful returns to depths of more than 50 m in carbonate sands.

A specially designed 24-channel hydrophone array receives the reflected energy from this source. It is constructed in three separate segments of eight channels each, with 1 m group intervals. This can produce the 0.5 meter along-track common depth points for signal stacking. The three-hydrophone groups are tightly spaced so that, while they effectively cancel random noise, no high frequency signal loss occurs at extreme angles of incidence. An Elics Delph24® processing system is used to receive and digitize the data. This system can sample 24 channels at 12 kHz, sufficient for anti-aliasing the broad-band Geopulse® signals.

Overall Assessment

Reduction of multi-channel seismic data for high resolution imaging is computationally intensive and not possible to complete in real-time or for a quick look given the hardware and personnel available for this project. Processing of the data has been initiated at MMTC/CSD, and will be reported independently to NFESC. Monitoring of the field acquisition showed that excellent data were collected. Field modifications in the system and favorable sea states combined to produce good conditions for the exercise.

REFERENCE CITED

Gerritsen, F. 1978. Beach and Surf Parameters in Hawai`i. University of Hawai`i Sea Grant Program Technical Report UNIHI-SEAGRANT-TR-78-02, 178 p.